

Supporting Information:

Belonging to

**Synthesis and Self-Assembly of Spin-Labile and Redox-Active Manganese(III)
Complexes**

Claudio Gandolfi, Tatiana Cotting, Paulo N. Martinho, Olha Sereda, Antonia Neels, Grace G.

*Morgan and Martin Albrecht**

Contents

1. Synthesis	S2
2. Magnetic measurements	S4
3. Langmuir films.....	S5
4. Crystallographic details	S9

1. Synthesis

General. The syntheses of 2,6-dihydroxybenzaldehyde was accomplished according to a published procedure,^{S1} all other reagents were commercially available and used as received. Flash chromatography was performed using silica gel 60 (63-200 mesh). All ¹H and ¹³C{¹H} NMR spectra were recorded at 25 °C on Bruker spectrometers and referenced to residual solvent ¹H or ¹³C resonances (δ in ppm, J in Hz). Assignments are based either on distortionless enhancement of polarization transfer (DEPT) experiments or on homo- and heteronuclear shift correlation spectroscopy. Melting points were determined using an OptiMelt apparatus (Stanford Research Systems) and are uncorrected. High resolution mass spectra were measured by electrospray ionization (ESI-MS) on a Bruker 4.7 T BioAPEX II. Elemental analyses were performed at the ETH Zurich (Switzerland).

Synthesis of 2a. To a solution of 2,6-hydroxybenzaldehyde (605 mg, 4.38 mmol) in DMF (8 mL) was added NaHCO₃ (368 mg, 4.38 mmol). After 10 min stirring at RT, 1-bromohexane (745 mg, 4.38 mmol) in DMF (8 mL) was slowly added. The mixture was heated to 120 °C for 4 h under Ar. After cooling to RT, aqueous HCl (1 M, 30 mL) was added and the mixture was vigorously stirred. The crude product was extracted with ethyl acetate (3 × 20 mL) and the combined organic phases were washed with brine (2 × 80 mL), dried over MgSO₄, and evaporated under reduced pressure. Purification by gradient column chromatography (SiO₂, hexane to hexane/ethyl acetate 15:1) gave **2a** as a pale yellow liquid (0.47 g, 41%). ¹H-NMR (CDCl₃, 360 MHz): δ 11.96 (s, 1H, OH), 10.37 (s, 1H, CHO), 7.39 (t, 1H, $J = 8.4$ Hz, C⁴H), 6.50, 6.36 (2 × d, 1H, $J = 8.4$ Hz, C³H and C⁵H), 4.03 (t, 2H, $J = 6.4$ Hz, OCH₂), 1.82 (m, 2H, OCH₂CH₂), 1.47 (m, 2H, OCH₂CH₂CH₂), 1.42–1.22 (m, 4H, CH₂), 0.91 (t, 3H, $J = 6.6$ Hz, CH₃). ¹³C-NMR (CDCl₃, 91 MHz): δ 194.6 (CHO), 163.7, 162.2 (2 × C_{Ar}-O), 138.6 (C⁴H), 111.0 (C_{Ar}-CHO), 109.6, 101.9 (C³H and C⁵H), 68.8 (OCH₂), 31.6, 29.1, 25.9, 22.7 (4 × CH₂), 14.1 (CH₃). HR-MS (ESI): calcd for C₁₃H₁₇O₃ [M - H]⁻ $m/z = 221.1183$, found $m/z = 221.1182$. Anal. found (calcd) for C₁₃H₁₈O₃(222.28): C 70.44 (70.25); H 8.22 (8.16).

S1 (a) S. Inoue, T. Yanai, S. Ando, A. Nakazawa, K. Honda, Y. Hoshino and T. Asai, *J. Mater. Chem.*, 2005, **15**, 4746. (b) P. Zell, F. Mögele, U. Ziener and B. Rieger, *Chem. Eur. J.*, 2006, **12**, 3847. (c) I. Aiello, M. Ghedini, M. La Deda, D. Pucci and O. Francescangeli, *Eur. J. Inorg. Chem.*, 1999, 1367.

Synthesis of 2b. According to the method described for **2a**, **2b** was obtained from 2,6-hydroxybenzaldehyde (552 mg, 4.00 mmol) and NaHCO₃ (336 mg, 4.00 mmol) in DMF (7 mL), and 1-bromododecane (1.03 g, 4.00 mmol) in DMF (7 mL). Column chromatography (SiO₂, pentane) yielded **2b** as a colorless solid (0.60 g, 49%). The product may be recrystallized from warm MeOH at -30 °C. M.p. 32 °C. ¹H-NMR (CDCl₃, 360 MHz): δ 11.96 (s, 1H, OH), 10.37 (s, 1H, CHO), 7.41 (t, 1H, *J* = 8.4 Hz, C⁴H), 6.50, 6.36 (2 × d, 1H, *J* = 8.4 Hz, C³H and C⁵H), 4.03 (t, 2H, *J* = 6.4 Hz, OCH₂), 1.82 (m, 2H, OCH₂CH₂), 1.46 (m, 2H, OCH₂CH₂CH₂), 1.40–1.16 (m, 16H, CH₂), 0.88 (t, 3H, *J* = 6.4 Hz, CH₃). ¹³C-NMR (CDCl₃, 91 MHz): δ 194.4 (CHO), 163.6, 162.1 (2 × C_{Ar}-O), 138.4 (C⁴H), 110.9 (C_{Ar}-CHO), 109.5, 101.7 (C³H and C⁵H), 68.7 (OCH₂), 32.0, 29.73, 29.71, 29.66, 29.63, 29.43, 29.40, 29.0, 25.9, 22.8 (10 × CH₂), 14.1 (CH₃). HR-MS (ESI): calcd for C₁₉H₂₉O₃ [M - H]⁻ *m/z* = 305.2122, found *m/z* = 305.2123. Anal. found (calcd) for C₁₉H₃₀O₃ (306.44): C 74.52 (74.47); H 9.82 (9.87).

Synthesis of 2c. According to the procedure described for **2a**, **2c** was obtained from 2,6-hydroxybenzaldehyde (552 mg, 4.00 mmol), NaHCO₃ (336 mg, 4.00 mmol), 1-bromooctadecane (1.37 g, 4.00 mmol) in DMF (total 14 mL). The crude product was extracted with CH₂Cl₂ (3 × 100 mL) and the combined organic phases were dried over MgSO₄, evaporated under reduced pressure and purified by gradient column chromatography (SiO₂, pentane), thus affording **2c** as an off-white solid (0.69 g, 44%). The product may be recrystallized from warm MeOH. M.p. 54 °C. ¹H-NMR (CDCl₃, 360 MHz): δ 11.96 (s, 1H, OH), 10.36 (s, 1H, CHO), 7.38 (t, 1H, *J* = 8.4 Hz, C⁴H), 6.50, 6.35 (2 × d, 1H, *J* = 8.4 Hz, C³H and C⁵H), 4.03 (t, 2H, *J* = 6.4 Hz, OCH₂), 1.82 (m, 2H, OCH₂CH₂), 1.46 (m, 2H, OCH₂CH₂CH₂), 1.40–1.14 (m, 28H, CH₂), 0.88 (t, 3H, *J* = 6.6 Hz, CH₃). ¹³C-NMR (CDCl₃, 91 MHz): δ 194.5 (CHO), 163.6, 162.1 (C_{Ar}-O), 138.4 (C⁴H), 111.0 (C_{Ar}-CHO), 109.5, 101.8 (C³H and C⁵H), 68.7 (OCH₂), 32.0, 30.0–28.5, 26.1, 22.7 (all CH₂), 14.2 (CH₃). HR-MS (ESI): calcd for C₂₄H₄₁O₃ [M - H]⁻ *m/z* = 389.3061, found *m/z* = 389.3066. Anal. found (calcd) for C₂₅H₄₂O₃ (390.61): C 77.10 (76.87); H 10.82 (10.84).

2. Magnetic measurements

Magnetic moments were calculated using the following equation:

$$\mu_{\text{eff}} = \sqrt{\left(\frac{3k_B}{N\mu_B^2}\right) (\chi_{\text{para}} T)} = 2.828 \sqrt{\chi_{\text{para}} T}$$

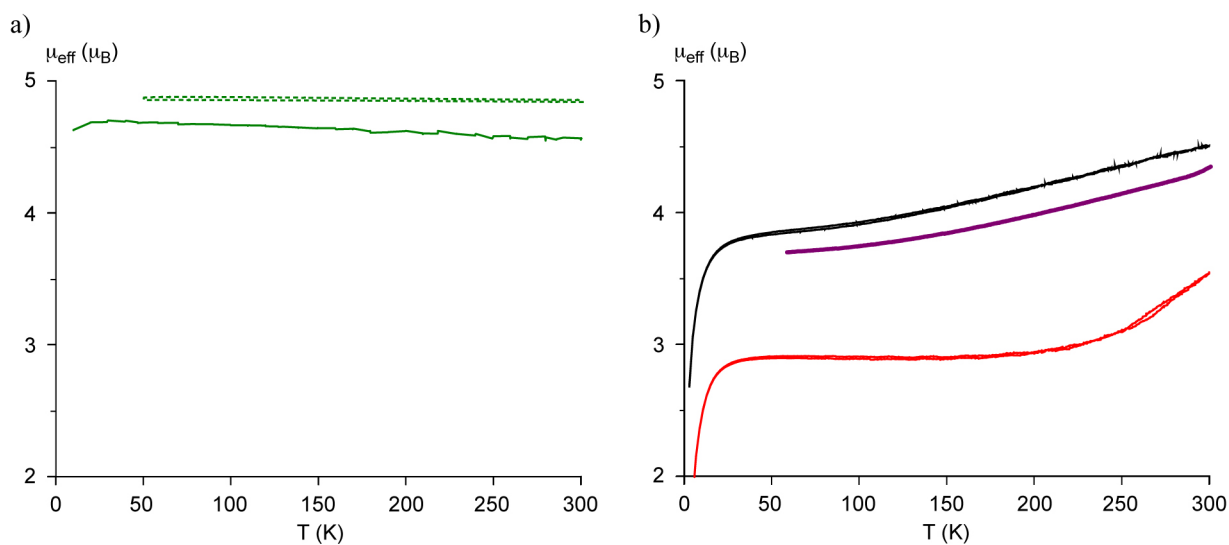


Figure S-1. Measurement of the temperature-dependent magnetic moment (a) of complexes **3a** (dashed) and **3c** (solid); (b) of complex **5c** as crystalline sample (red), pre-heated to 350 K (purple), and as powder (black).

3. Langmuir films

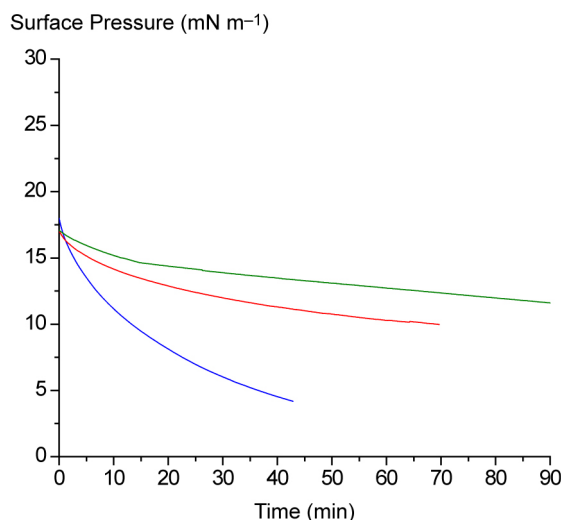


Figure S-2. Film stability over time of monolayers composed of **3b** (green), **4b** (blue), and **5b** (red).

Transfer of Langmuir films on support

Monolayers of complexes **3c**, **5c**, and **5b** were transferred on glass wafers by the vertical dipping method in order to fabricate LB multilayers (Table S-1).^{S2} When using monolayers composed of **3c**, the first three layers were deposited with acceptable transfer ratios during upstroke (Fig. S-3a). However, the downstroke transfer ratios were close to zero, indicating that immersion did not result in film transfer and hence, a Z-type LB multilayer is obtained. The third downstroke revealed a negative transfer ratio, indicating that the previously adsorbed layer was partially desorbed again. This process was even more evident in subsequent cycles, where up- and downstroke transfer ratios were equal but with opposite signs, thus indicating complete removal of the adsorbed layer during downstroke. Obviously, such behavior impedes the deposition of further layers.

S2 Multilayer LB depositions were carried out by the vertical dipping method onto glass substrate, after holding the monolayer at a constant surface pressure of 4 mN/m and allowing the monolayer to equilibrate for 10 min. The dipper speed was maintained at 4 mm/min for upward and downward motion. Before each downstroke the wafer was allowed to dry for 20 min in air.

Table S-1. Transfer ratio of multilayer deposition onto a glass support^a

Layer number	3c	5c	5b
1	0.76	0.85	0.58
2	0.04	-0.34	-0.30
3	0.44	0.56	0.41
4	-0.10	-0.31	-0.31
5	0.58	0.51	0.39
6	-0.37	-0.29	-0.35
7	0.61	0.48	0.38
8	-0.59	-0.26	-0.33
9	0.66	0.46	0.36
10	-0.65	-0.23	-0.31
11	0.66	0.43	0.35

^a glass area approximately 2.4 x 2.4 cm² (2.4 x 1.26 cm² when immersed), transfer at surface pressure = 4 mN m⁻¹, drying time before immersion (even layer numbers) = 20 min.

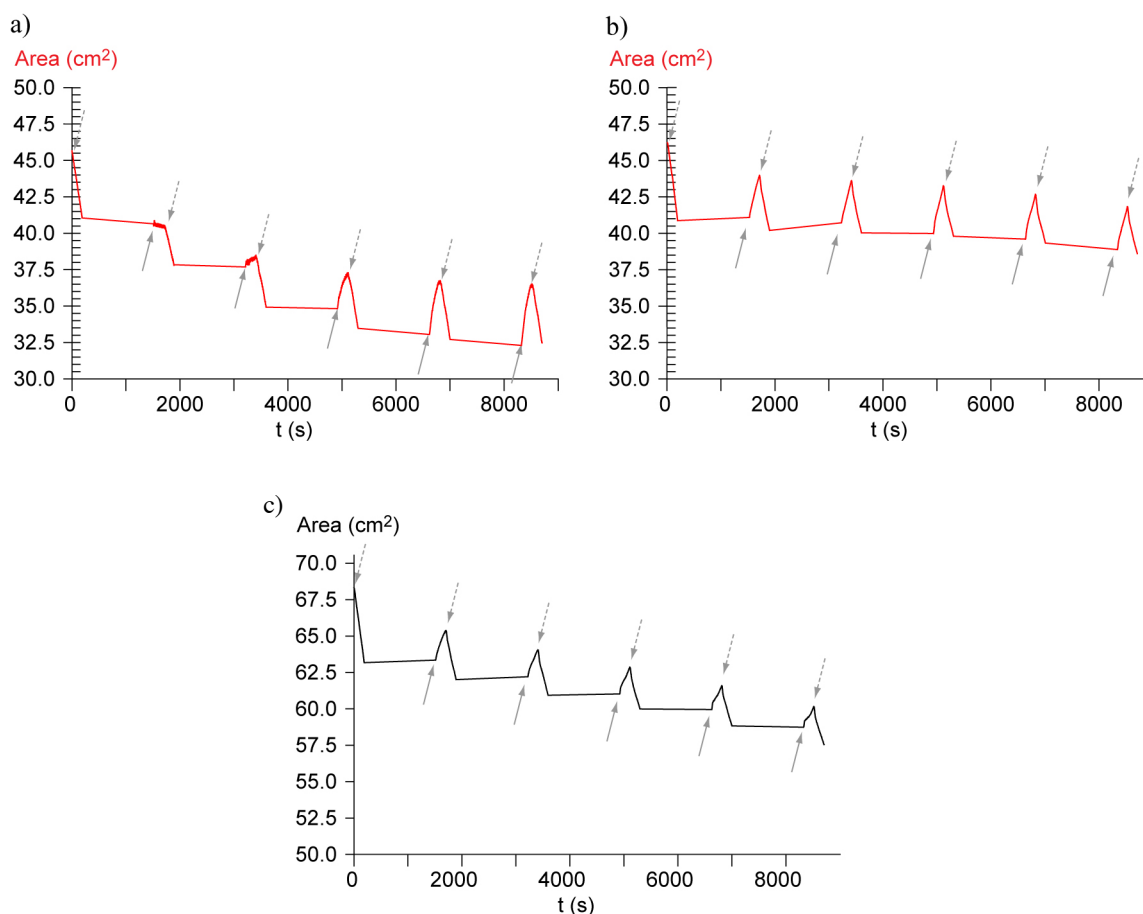


Figure S-3. Langmuir film transfer of **3c** (a), **5b** (b), and **5c** (c) onto a glass wafer at surface pressure 4 mN m⁻¹ and dipping rate 4 mm min⁻¹ (transferred area in red, dashed arrows indicate start of upstroke, solid arrows start of downstroke after the wafer was dried in air for 1200 s).

Slightly improved transfer characteristics were observed for monolayers composed of the manganese sal₂bapen complex **5c** (Fig S-3c). While already the first layer was partially removed upon downstroke (transfer ratio -0.34 vs. +0.85 during upstroke), the adsorption/desorption ratio in subsequent cycles remained around 2:1. Hence, material was continuously deposited onto the wafer. However, the fact that only partial film transfer occurred already at an early stage suggests that ill-defined layers were formed, thus derogating the reproducibility and also the predictable behavior of multilayered assemblies. These drawbacks are particularly relevant when aiming at constructing true devices.

When monolayers of **5b** containing shorter dodecyl chains were used for LB film fabrication, only a single layer was deposited (Fig. S-3b). In subsequent cycles, the upstroke process completely removed the adsorbed layer again. Apparently, the hydrophilic-hydrophobic balance requires further refinement for multilayer deposition. Perhaps, the increased lipophilicity of the sal₂bapen scaffold as compared to the sal₂trien ligand reduces the affinity of the head group to the glass wafer and thus decreases the stability of the deposited films, leading to high desorption ratios.

Apparently, there is a high propensity for this type of complex to form Z-type LB films, irrespective of the ligand setup and the metal center (Mn³⁺, Fe³⁺, and Co³⁺). Deposition of several Langmuir monolayers is precluded because of partial desorption, which might originate from disorder in the adsorbed layers.^{S3} Such disorder is expected to increase with the number of deposited layers. Generally, Z- or X-type LB films are less stable than Y-type films and tend to form with head groups that are not particularly hydrophilic.^{S4}

S3 M. Li, X.-H. Li, L. Huang, Q.-J. Jia, W.-L. Zheng and Z.-H. Mai, *Europhys. Lett.*, 2003, **64**, 385.

S4 K. Fukuda and T. Shiozawa, *Thin Solid Films*, 1980, **68**, 55.

UV-vis analysis of LB-films

Since the low quantity of deposited material precluded magnetic measurements of the LB films, we concentrated on UV-vis spectroscopic analysis. At RT the LB film obtained from **5c** showed two absorbance bands at 448 nm and at 494 nm, and a broad and weak band centered at about 570 nm (Fig. S-4). The first two bands are better resolved than in solution and may correspond to the MLCT band at 504 nm observed in CH_2Cl_2 . Gradual decrease of the temperature to 92 K did not result in significant changes in the absorption spectrum, though even in the bulk, the color change has been noted to be only marginal (see main text).

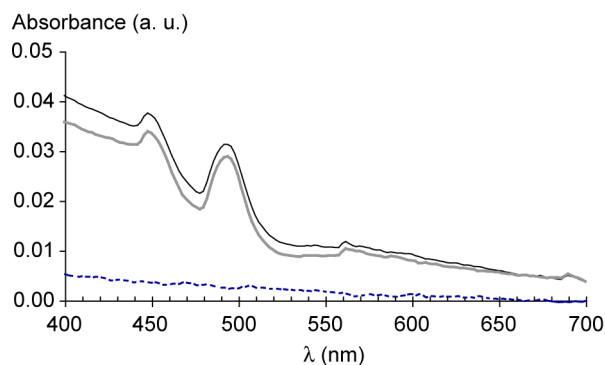


Figure S-4. UV-vis spectra at LB-monolayer of **5c** at 298 K (bold), 92 K (solid), and the corresponding difference spectra (dashed).

4. Crystallographic details

Table S-2. Bond Angles (°) around the Manganese Center in Complexes **3a**, **4a**, and **5a**.

	3a × 1.75 H ₂ O		4 × 0.75 acetone		5 × H ₂ O
	M = Mn1	M = Mn2	M = Mn1	M = Mn2	M = Mn1
O1–M–O2	105.3(4)	105.0(4)	178.7(3)	177.8(3)	179.68(10)
O1–M–N1	88.4(4)	89.7(5)	88.6(3)	88.1(3)	87.42(10)
O1–M–N2	161.2(4)	164.0(5)	94.2(3)	96.3(3)	93.24(10)
O1–M–N3	88.1(4)	90.2(5)	87.1(3)	87.6(3)	85.62(10)
O1–M–N4	93.8(5)	94.7(5)	92.9(3)	92.8(3)	92.76(11)
O2–M–N1	91.1(4)	90.7(5)	92.7(3)	90.6(3)	92.83(11)
O2–M–N2	90.3(4)	88.5(4)	86.3(3)	85.4(3)	86.58(10)
O2–M–N3	164.4(5)	162.6(5)	91.8(3)	94.1(3)	94.10(10)
O2–M–N4	89.5(5)	89.7(4)	86.4(3)	86.0(3)	87.37(11)
N1–M–N2	80.7(4)	81.6(5)	85.0(3)	84.2(4)	86.39(11)
N1–M–N3	97.2(5)	97.9(6)	164.5(3)	163.2(3)	165.93(11)
N1–M–N4	177.4(5)	175.4(5)	110.2(3)	113.0(4)	104.66(12)
N2–M–N3	78.1(4)	77.9(5)	80.6(3)	80.2(3)	81.82(9)
N2–M–N4	96.8(5)	93.8(5)	163.4(3)	160.9(3)	167.65(11)
N3–M–N4	81.6(6)	80.5(5)	84.9(3)	83.5(3)	87.89(10)

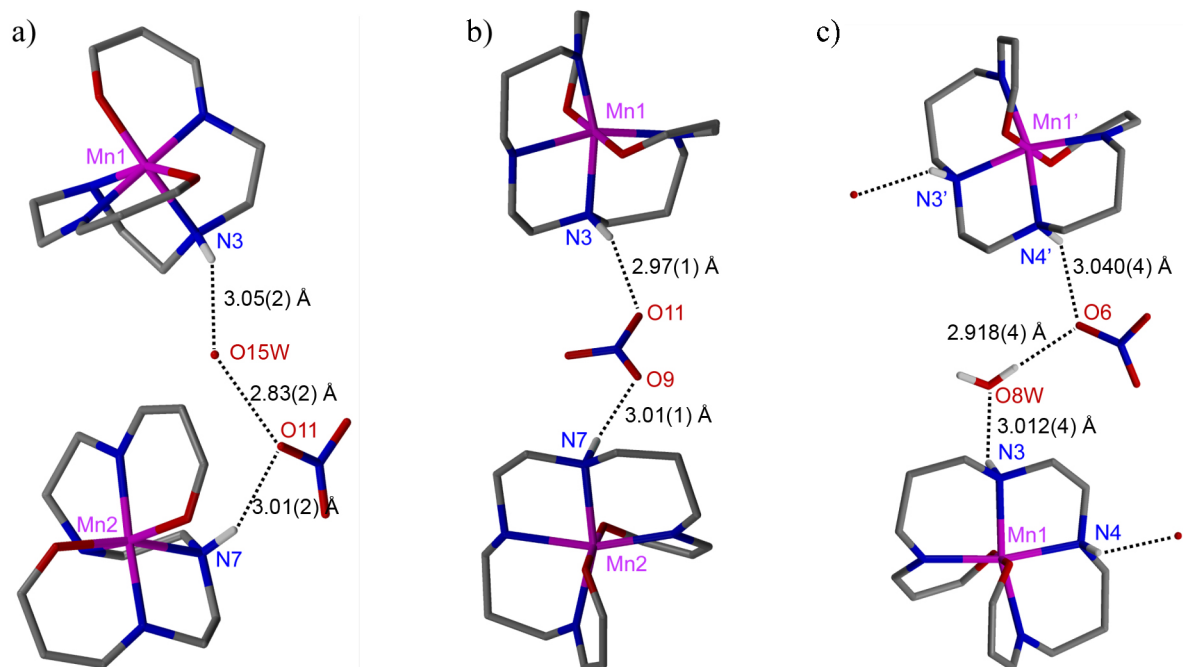


Figure S-5. Hydrogen bonding in complexes **3a-5a**. Dimeric structures formed by hydrogen bonding of two crystallographically independent complex cations in structures **3a** (a) and **4a** (b), and the polymeric structure of **5a** (c; a prime denotes symmetry operation $\frac{1}{2}-x, \frac{1}{2}+y, \frac{1}{2}-z$; aromatic rings and hexyloxy groups of all complexes and irrelevant hydrogen atoms not shown).

Table S-3. Crystallographic Data for Complexes **3a**, **4a**, and **5a**.

	3a	4a	5a
color, shape	yellow, plate	yellow, plate	orange, rod
crystal size/mm	0.50 × 0.50 × 0.20	0.50 × 0.25 × 0.15	0.45 × 0.25 × 0.10
empirical formula	C ₃₂ H ₄₈ MnN ₅ O ₇ × 1.75 H ₂ O	C ₃₄ H ₅₂ MnN ₅ O ₇ × 0.75 C ₃ H ₆ O	C ₃₄ H ₅₂ MnN ₅ O ₇ × H ₂ O
Fw	701.22	741.30	715.76
T/K	173(2)	173(2)	173(2)
crystal system	monoclinic	orthorhombic	monoclinic
space group	<i>P</i> 2 ₁ (No. 4)	<i>Pca</i> 2 ₁ (No. 29)	<i>P</i> 2 ₁ / <i>n</i> (No. 14)
unit cell			
<i>a</i> /Å	20.6789(18)	15.997(3)	13.9091(7)
<i>b</i> /Å	7.4435(4)	14.451(4)	10.9326(7)
<i>c</i> /Å	25.026(2)	33.798(7)	24.2850(14)
<i>α</i> /deg	90	90	90
<i>β</i> /deg	106.542(7)	90	90.880(4)
<i>γ</i> /deg	90	90	90
<i>V</i> /Å ³	3692.7(5)	7813(3)	3692(4)
<i>Z</i>	4	8	4
<i>D</i> _{calc} /g cm ⁻³	1.261	1.260	1.288
<i>μ</i> /mm ⁻¹ (Mo K _α)	0.412	0.391	0.412
no. of total, unique reflns	19772, 11368	38140, 10212	24062, 6975
<i>R</i> _{int}	0.1201	0.1389	0.0669
transmission range	–	0.865–0.926	0.871–0.903
no. parameters, restraints	734, 16	670, 30	429, 3
<i>R</i> , <i>R</i> _w ^a	0.1163, 0.3279	0.0528, 0.1102	0.0527, 0.1242
GOF	0.963	0.621	0.874
min,max resid density/e Å ⁻³	–0.472, 0.973	–0.338, 0.272	–1.040, 1.231

^a $R_1 = \Sigma ||F_o| - |F_c|| / \Sigma |F_o|$ and $wR_2 = [\Sigma w(F_o^2 - F_c^2)^2 / \Sigma w(F_o^4)]^{1/2}$ for all $I > 2\sigma(I)$